Physical Parameters That Control the Imaging of Purple Membranes with the Scanning Tunneling Microscope

R. García* and J. Tamayo

Centro Nacional de Microelectrónica, CSIC, Serrano 144, 28006 Madrid, Spain

J. M. Soler

Departamento de Física Materia Condensada, C-III, Universidad Autónoma de Madrid, 28049 Madrid, Spain

C. Bustamante

Institute of Molecular Biology, University of Oregon, Eugene, Oregon 97403

Received August 2, 1994. In Final Form: January 23, 1995[⊗]

The dominant physical and geometrical parameters for imaging hydrated purple membranes with the scanning tunneling microscope are identified and characterized. These are sample voltage, current density, and tip radius. Purple membranes are imaged with vertical and lateral resolution of 0.7 nm and 15 nm, respectively. We also found that the apparent height of the membranes depends on the tip–substrate separation. These experiments pose the problem of electron transport through 5–10 nm thick insulating materials. We propose a model where the contrast mechanism is controlled by two factors, the electric field at the interface and the transmission through empty states in the membrane.

I. Introduction

The scanning tunneling microscope (STM) is a powerful tool for imaging[1] and modification[2] of metallic, semimetallic, and semiconductor surfaces at atomic and nanometer scales. The operation of the STM is not restricted to ultrahigh vacuum. Atomic resolution images can be obtained in air and under liquid environments as well.

Direct three-dimensional imaging, atomic resolution, and operating under water have prompted the application of STM for imaging biomolecules. For a biologist, these experiments open the possibility of imaging biomolecules in conditions close to physiological ones. From physicist and chemist's points of view, they may offer unique possibilities for measuring electrical conductivities and studying mechanisms of electron transport in such complex systems. At the interface of physics, chemistry, and biology, they would provide methods to manipulate and incorporate biomolecules into new physical devices as biosensors.

A wide variety of organic and biological molecules have been examined by STM,[3] liquid crystals,[4] long chain *n*-alkanes,[5] Langmuir–Blodget films[6] to mention only a few studies involving organic macromolecules. DNA bases,[7] DNA,[8] DNA–protein complexes,[9] globular and elongated proteins,[10,11] and several protein membranes[12–15] are examples of biomolecules studied by STM. Those experiments have to deal with the potential problems associated with the poor electrical conductivity of macromolecules. They also pose the problem of the contrast mechanism that allows imaging by STM.

For very thin organic films (say below 1 nm) several models and calculations based on the coupling between substrate and molecule orbitals,[16] resonant tunneling,[17] or the modulation of the effective barrier by polarizable molecular adsorbates[4] give reasonable explanations of the observed contrast. The situation is more complicated when larger macromolecules are involved and direct tunneling through them gives a negligible contribution to the total current. The experiments themselves are somehow controversial. In some cases images have been difficult to reproduce and the factors that contribute to imaging were not properly isolated. In this respect, it is illustrating the case of STM images of DNA.[18] On the other hand, the electrical conductivities of some organic films implied by STM observations ($\sim 10^{-2}\ \Omega^{-1}\ cm^{-1}$) are several orders of magnitude higher than previous macroscopic measurements.[19–21] In general, the mechanism

[⊗] Abstract published in *Advance ACS Abstracts,* April 1, 1995.

(1) *Scanning Tunneling Microscopy*; Güntherodt, H.-J., Weisendanger, R., Eds.; Springer Verlag: Berlin, 1991; Vol. 1–2, and references therein.

(2) For a collection of recent papers, see Atomic and Nanometre-scale modification of materials: Fundamentals and applications. *NATO ASI Ser., Ser. E.* **1993**, *No. 239*.

(3) *STM and SEM in biology*; Marti, O., Amrein, M., Eds.; Academic Press Inc.: San Diego, CA, 1993; and references therein.

(4) Spong, J. K.; Mizes, H. A.; LaComb, L. J., Jr.; Dovek, M. N.; Frommer, J. E.; Foster, J. S. *Nature* **1989**, *338*, 137.

(5) Rabe, J. P.; Buchholtz, S. *Phys. Rev. Lett.* **1991**, *66*, 2096–2099.

(6) Smith, D. D.; Bryant, A.; Quate, C. F.; Rabe, J. P.; Gerber, Ch.; Swalen, J. P. *Proc. Natl. Acad. Sci. U.S.A.* **1987**, *84*, 969.

(7) Tao, N. J.; DeRose, J. A.; Lindsay, S. M. *J. Phys. Chem.* **1993**, *97*, 910.

(8) Beebe, T. P.; Wilson, T. E.; Ogletree, F. D.; Katz, J. E.; Balhorn, R.; Salmeron, M. B.; Siekhaus, W. J. *Science* **1989**, *243*, 370–372.

(9) Amrein, M.; Durr, R.; Stasiak, A.; Gross, H.; Travaglini, G. *Science* **1989**, *243*, 1708.

(10) Welland, M. E.; Miles, M. J.; Lambert, N.; Morris, V. J.; Coombs, J. H.; Pethica, J. B. *Int. J. Biol. Macromol.* **1989**, *11*, 29.

(11) Miles, M. J.; Carr, H. J.; McMaster, T. J.; I'Anso, K. J.; Belton, P. S.; Morris, V. J.; Field, J. M.; Shewry, P. R.; Tatham, A. S. *Proc. Natl. Acad. Sci. U.S.A.* **1991**, *88*, 68–71.

(12) Guckenberger, R.; Wiegrabe, W.; Hillerbrand, A.; Hartmann, T.; Wang, Z.; Baumeister, W. *Ultramicroscopy* **1989**, *31*, 327–332.

(13) Hörber, J. K. H.; Schuler, F. M.; Witzemann, V.; Schröter, K. H.; Müller, H.; Ruppersberg, J. P. *J. Vac. Sci. Technol. B* **1991**, *9*, 1214.

(14) Bertazzon, A.; Conti-Tronconi, B. M.; Raftery, M. A. *Proc. Natl. Acad. Sci. U.S.A.* **1992**, *89*, 9632.

(15) Niemi, H. E. M.; Ikonen, M.; Levlin, J. M.; Lemmetyinen, H. *Langmuir* **1993**, *9*, 2436.

(16) Smith, D. P. E.; Hörber, J. K. H.; Binnig, G.; Nejoh, H. *Nature* **1990**, *344*, 641–644.

(17) Mizutami, W.; Shigeno, M.; Ono, M.; Kajimura, K. *Appl. Phys. Lett.* **1990**, *56*, 1974.

(18) Dunlap, D.; García, R.; Schabtach, E.; Bustamante, C. *Proc. Natl. Acad. Sci. U.S.A.* **1993**, *90*, 7652–7655.

(19) Eley, D. D.; Spivey, D. I. Semiconductivity of organic substances: Nuclei acid in dry state. *Trans. Faraday Soc.* **1962**, *58*, 411.

(20) Mann, B.; Kuhn, H. *J. Appl. Phys.* **1971**, *42*, 4398.

0743-7463/95/2411-2109$09.00/0

of conductivity operating in STM experiments involving several nanometer thick macromolecules is not known.

Guckenberger et al. have shown that high-resolution and reproducible images of several uncoated protein membranes can be achieved by operating the STM at relatively high voltages and very low currents.[12,22] Here, high voltages and low currents mean those above 5 V and below 1 pA, respectively. However, the relevant imaging conditions were not fully described. Moreover, the physical processes responsible for the conductivity remain unknown.

In this paper, we apply Guckenberger's approach to study the geometrical and electrical parameters that control the imaging of purple membranes by STM. On the basis of the experimental results, we propose a model where the imaging mechanism is controlled by the electrical field at the interface and the existence of empty electronic states in the membrane.

II. Materials and Methods

Purple membrane (PM) is the biological system chosen in this study. PM is a natural membrane crystal present in the cell membrane wall of halobium bacteria. The membranes used in this study have been obtained following the procedure described in ref 23. Its structure has been characterized by electron microscopy and diffraction[24] and recently by atomic force microscopy.[25,26] The purified membranes appear as oval sheets of about 1 μm diameter and about 4.5–5 nm thickness.

PM is made of a single protein species, bacteriorhodopsin. The proteins are packed in hexagonal symmetry, space group $p3$, with lattice parameter 6.3 nm. Biologically, the protein acts as a light-driven proton pump. Due to its structural stability in a wide range of environmental conditions and its remarkable optical properties, PM is drawing interest for its potential applications as a high-performance component of optical computers.[27]

Highly oriented pyrolitic graphite (HOPG) is used as a solid, conductive support (substrate) for the membranes. It has several convenient features. HOPG has been extensively studied by STM. It is easily cleaved and inert, offering large, atomically flat areas for deposition. In addition to the above properties, graphite has no structural defects that could resemble the membranes shape.

Approximately 10 μL of an aqueous suspension of PM (0.1 mg/mL) is sprayed onto the substrate. The graphite is placed perpendicular to the stream and about 10 cm away from the atomizer. The spreading produces small droplets on the graphite that rapidly evaporate, leaving the PM on the surface. The process is repeated several times to guarantee a uniform coverage of the surface.

Without any further preparation the sample is loaded into a special STM chamber that allows control of the relative humidity from 5 to 100%. The images are taken in the constant current mode with a low current STM described elsewhere.[28] Set currents as small as 0.1 pA can routinely be measured while scanning at speeds of 1 scan line/s. This means that each data point is an average over 10^3 electrons. This effectively will minimize the interaction between the molecules and the electron beam. As a comparison, in standard STM experiments 10^7 electrons are collected for each data point. The images presented here are raw data with no other filtering than the substraction of the background plane.

A relevant factor for imaging biomolecules is the geometry of the tip. Platinum–iridium electrochemically etched tips have been used.[29] These tips have a high aspect ratio. For some of them, curvature radii as small as 10 nm were measured.

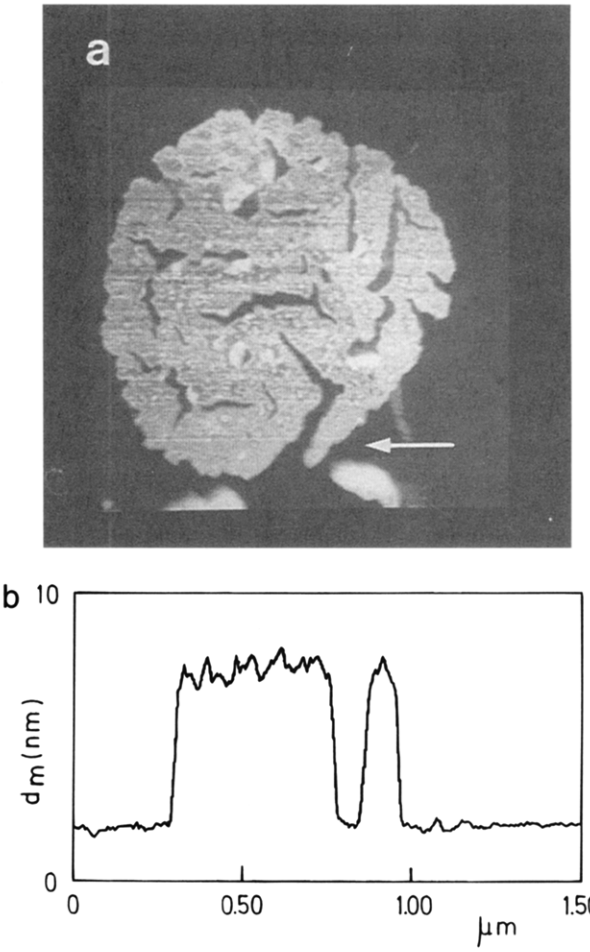

Figure 1. (a) Topographic STM image of a hydrated purple membrane deposited on HOPG: scan size, 1.69 μm × 1.69 μm; sample voltage, −7.7 V; tunneling current, 0.2 pA; relative humidity, 41%. Several cracks occurring while air-drying are visible. (b) Cross section along the line marked by an arrow in (a).

III. Results and Discussion

Figure 1 is a topographic image of an uncoated PM sheet on HOPG. The STM current, I, and applied voltage, V, are 0.2 pA and −7.7 V (sample negative), respectively. At the scale of the image, no details of the crystalline structure are visible. Under the present imaging conditions the estimated lateral resolution is about 15 nm. This value is deduced by measuring the width of the cracks occurring while slow air-drying of the membranes. Those cracks show angles of 60° or 120° that reflect the hexagonal symmetry of the membrane. Cross sections as the one shown in Figure 1b allow height measurements. The membrane protrudes from the HOPG surface 5.2 ± 0.4 nm, i.e., in close agreement with previous measurements by other techniques.[24] However, in general, the apparent height of the membrane will depend on the initial tip–substrate separation. This aspect will be discussed in next section.

The operation of the STM at relatively high voltages (it has been called near field emission regime[30]) allows an

(21) García, R.; Dunlap, D.; Bustamante, C. Scanning Probe Microscopies II. *Proc. SPIE* **1992**, *1855*, 2–11.
(22) Guckenberger, R.; Hacker, B.; Hartmann, T.; Scheybani, T.; Wang, W.; Wiegräbe, W.; Baumeister, W. *J. Vac. Sci. Technol. B* **1991**, *9*, 1227.
(23) Oesterhelt, D.; Stoeckenius, W. *Methods Enzymol.* **1974**, *31*, 667–678.
(24) Henderson, R.; Unwin, P. N. T. *Nature* **1975**, *257*, 2832.
(25) Worcester, D. L.; Kim, K. S.; Miller, R. G.; Bryant, P. J. *J. Vac. Sci. Technol. A* **1990**, *8*, 403–405.
(26) Butt, H. J.; Prater, C. B.; Hansma, P. K. *J. Vac. Sci. Technol. B* **1991**, *9*, 1193.
(27) Haronian, D.; Lewis, A. *Appl. Opt.* **1991**, *30*, 597–608.
(28) Dunalp, D.; Smith, S.; Bustamante, C.; Tamayo, J.; García, R. Submitted for publication in *Rev. Sci. Instrum.*

(29) Pt–Ir etched tips were manufactured by Materials Analytical Services, Raleigh, NC.

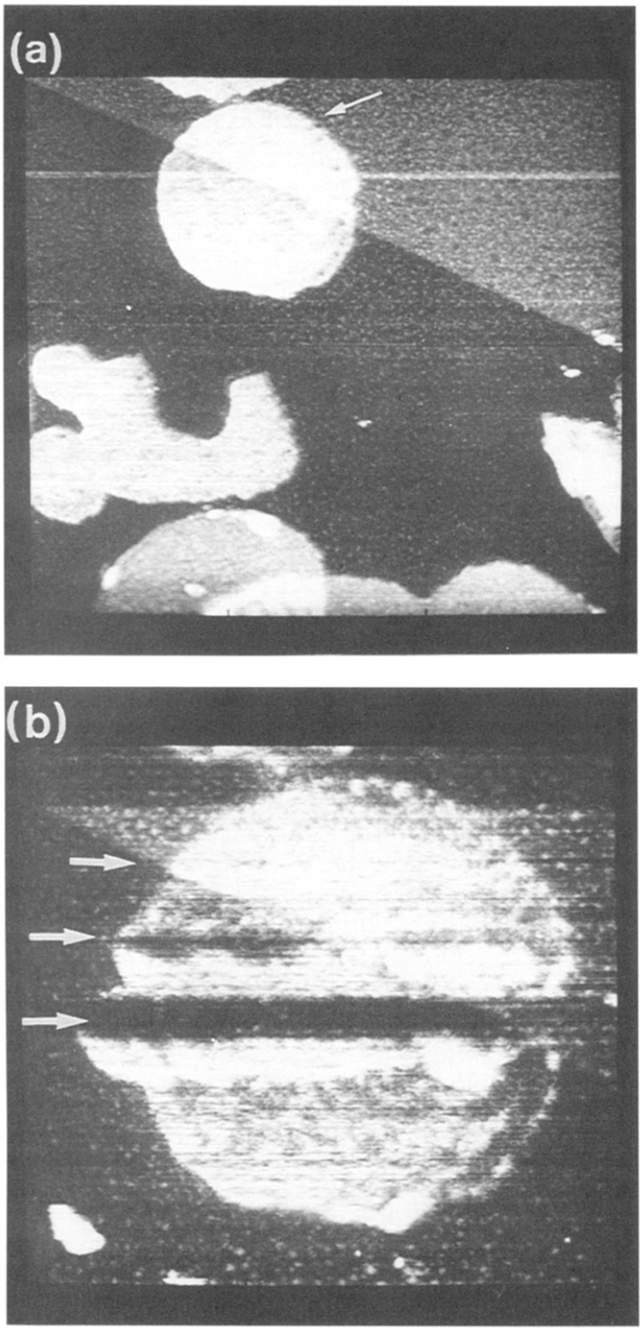

Figure 2. Voltage dependence. (a) STM image of several PM on HOPG (3 μm × 3 μm). At the bottom, the partial overlapping of two membranes can be seen. This implies electron transport through 10 nm of proteins. A monoatomic step of carbon atoms tranversally crosses the image. It effectively anchors the membrane to the substrate. Sample bias was −7.3 V. (b) Three different regions of the membrane marked by an arrow in Figure 2a scanned at −6, −5 V, and −4 V, respectively (top to bottom). The image has been taken at −6.6 V. Tunneling current was 0.15 pA and relative humidity was 25%. Scan size was 1.34 μm × 1.34 μm.

estimation of the tip−substrate separation. The tip's displacement is recorded when the applied voltage is ramped from say −7 to −0.1 V while the current is kept constant. In this way, for an initial gap distance defined by $I = 0.1$ pA and $V = -7$ V, tip displacements of about 6 nm have been measured. This means that the membranes are imaged in a noncontact mode. This in turn will minimize any distortion in the membrane due to interaction forces with the tip.

Figure 2a shows several PMs ($I = 0.16$ pA and $V = -7.3$ V). The partial overlapping of two membranes can be seen at the bottom. This implies electron transport through 10 nm of proteins. The membranes are anchored by structural defects in the substrate, such as steps. This is illustrated in Figure 2a, where a monoatomic step can be seen running transversally underneath a membrane.

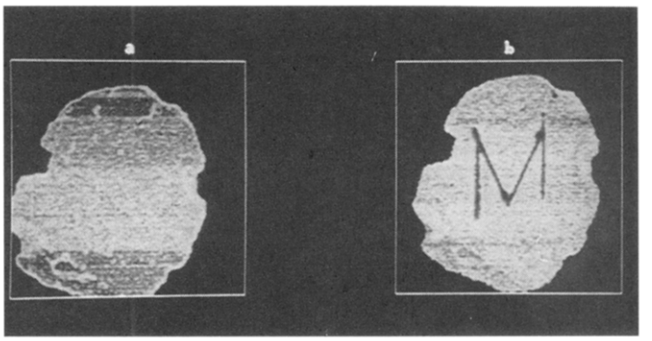

Figure 3. Current dependence experiments: (a) STM image of a purple membrane; (b) image after a pattern has been impressed in the membrane. The pattern is generated by scanning at 20 pA. It implies the removal of the proteins in the modified region. In (a) and (b), sample voltage was −7.7 V, tunneling current was 0.2 pA, and relative humidity was 37%. Scan size was 1.24 μm × 1.24 μm.

For study of the influence of the applied voltage in the imaging conditions, three separated regions of about 50 nm width have been scanned at −6, −5, and −4 V, respectively (Figure 2b). At −6 V there are not any noticeable effects. However, the region scanned at −5 V shows the partial removal of the proteins. This effect is more dramatic when the applied voltage is lowered at −4 V. All the proteins of the scanned region have been removed from it. They are seen piled up to the sides of the stripped region.

The explanation of this behavior is straightforward. At low voltages, not enough electrons flow from the sample to tip to sustain the set current. In order to keep the current constant, the tip approaches the sample until it makes mechanical contact with it. The depth of the contact depends on the voltage. At −4 V the tip has penetrated the full thickness of the membrane. The threshold voltage that separates noncontact imaging from contact is 5.5 ± 0.5 V. The dispersion from the mean value is tip dependent.

Though purple membranes can be imaged at both voltage polarities, better results are obtained when the substrate is biased negative with respect to the tip. In particular, resolution is better for that polarity because tip−substrate distances are smaller. Furthermore, ocassional fragmentation of PM has been observed when electrons are emitted from the tip. This is reminiscent of the process described for dissociating decaborane molecules.[31]

An equivalent experiment is performed for determining the dependence of image quality on the current. The PM shown in Figure 3a has been imaged at $I = 0.2$ pA and $V = -8$ V. The pattern in Figure 3b has been generated by scanning that region at 20 pA while keeping the voltage at −8 V. Operation of the STM at 20 pA produces the total removal of the proteins in the scanned region. Further experiments have determined that no more than 2 ± 1 pA can be carried through the membrane before tip−sample contact takes place. This current is distributed over an area πr^2, where r is defined by the effective lateral spatial resolution ($r = L_{\text{eff}}/2$). This amounts to a current density of 0.64 A/cm^2, i.e., 5 orders of magnitude

(30) Sáenz, J. J.; García, R. *Appl. Phys. Lett.* **1994**, *65*, 3022.
(31) Dujardin, G.; Walkup, R. E.; Avouris, Ph. *Science* **1992**, 1232–1235.

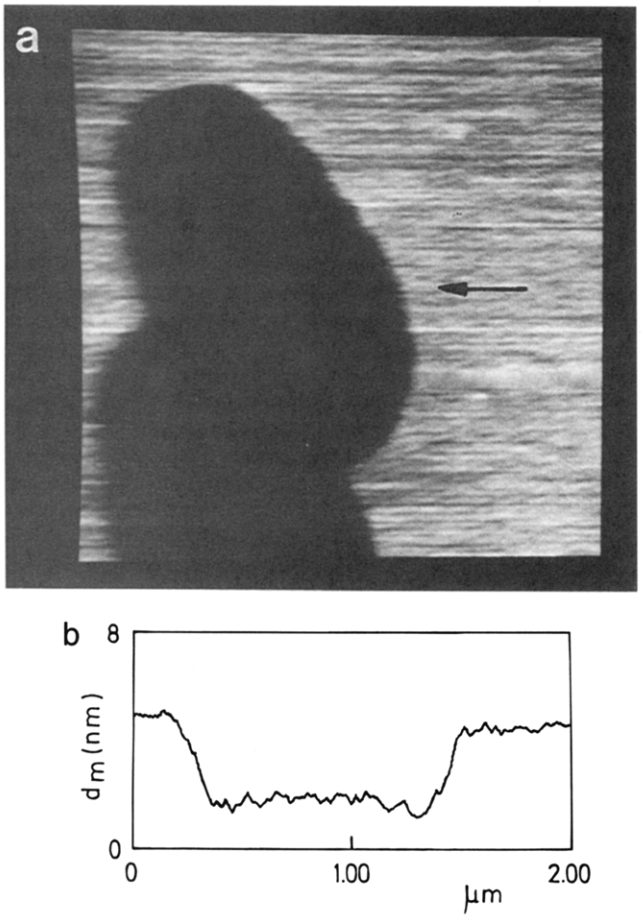

Figure 4. (a) Negative contrast STM images of purple membranes. To keep the current constant the tip approaches toward the membrane. This approach is larger in the overlapping region. (b) Cross section along the line indicated by the arrow in (a), $d_m \approx -3$ nm. $I = 0.09$ pA and $V = -6$ V.

smaller than the current densities measured in STM experiments on metallic or semiconductor surfaces.

Figure 3b also shows the potential of the STM as a dual purpose tool, for imaging and nanometer-scale modification of biomolecules.[32] The letter written on the membrane has a line with an average width 15 nm.

Figure 4 illustrates another feature sometimes observed while imaging bare biomolecules with the STM. The PM appears as a depression instead of protruding from the substrate surface. This is called negative contrast. This effect has also been reported in previous experiments with PM[22] and imaging DNA deposited onto chemically modified gold surfaces.[33]

Negative contrast in an example of how electronic effects appear in a STM topograph. A behavior that was predicted in one of the earliest reports about STM.[34] In this case, it implies that for a given tip–support separation (always higher than the thickness of the membrane) the effective gap resistance when the tip is over the PM is higher than that when the tip is over the substrate. In the constant current mode, this is compensated by a reduction of the tip–sample distance when the tip moves from bare graphite to the membrane (between 1 and 4 nm). Negative contrast implies extremely large tip–substrate separations (above 10 nm), so there is no mechanical contact when the tip approaches toward the membrane. Negative contrast is also accompanied by absence of any features within the membrane. Some contributions to the observed contrast could come from tip-induced deformations of the membrane. However, the observation of PM by AFM, where larger forces may be present, indicates that force deformations are not a dominant factor for negative contrast.

This anomalous behavior appears to be related to the geometry of the tip. We have measured the curvature radius of ten different tips by scanning electron microscopy. Five of them generated negative contrast while the other five gave positive contrast. The tips that produce negative contrast have consistently larger radii than their counterparts. In all the cases examined, positive contrast was obtained with tips of curvature radius smaller than 50 nm. An explanation of negative/positive contrast images will be provided in the next section.

The PM is better observed for relative humidities between 15 and 60%. The upper limit is imposed by the condensation of water vapor at high relative humidities on the microscope insulating components. This produces leakage currents and reduces considerably the signal-to-noise ratio. At low relative humidities there is a partial fading of the membranes in the image. The origin of this effect is not clear yet. We speculate that could be related to changes in the dielectric response of the membrane with water absorption.

IV. Contrast Mechanism

Several models have been proposed for explaining STM experiments of biomolecules: conduction enhancement by energy relaxation in disordered systems,[35] pressure induced resonant tunneling,[36] impurity-mediated electronic conduction,[37] and ion assisted conduction.[38]

The calculations of García and García[35] have been developed for low voltages (less than 1 V) and cannot fully describe the processes occurring at high voltages. The mechanism of conduction proposed by Lindsay et al.[36] explicitly invokes mechanical contact as a way to induce electronic resonances. We have shown that proper imaging of PM is only possible when there is no mechanical contact.

In these experiments, we have used purified PM crystals that have a well-defined and established composition. Other macromolecules have been imaged[12,22] utilizing physical parameters similar to those used here. These observations seem to exclude an electric-field-induced, impurity-mediated process. Furthermore, pulsing currents associated to the mechanism proposed by Tang et al. to explain experiments with hydroxy propyl cellulose films[37] have not been observed here.

To further characterize the mechanism of image formation, I versus V curves have been measured. These experiments are performed by holding the tip over the sample at a fixed position. Then, the voltage is ramped and simultaneously the current is measured. A typical curve is presented in Figure 5. This curve has been taken in a region of the substrate adjacent to a PM sheet.[39]

(32) García, R. *Appl. Phys. Lett.* **1994**, *64*, 1162. Tamayo, J.; Sáenz, J. J.; García, R. *J. Vac. Sci. Technol. A*, in press.
(33) Allison, D. P.; Bottomly, L. A.; Thundat, T.; Brown, G. M.; Woychik, R. P.; Schrick, J. J.; Jacobson, K. B.; Warmack, R. J. *Proc. Natl. Acad. Sci. U.S.A.* **1992**, *89*, 10129–10133.
(34) Binnig, G.; Rohrer, H.; Gerber, Ch.; Weibel, E. *Phys. Rev. Lett.* **1983**, *50*, 20.
(35) García, R.; García, N. *Chem. Phys. Lett.* **1991**, *173*, 44–50.
(36) Lindsay, S. M.; Sankey, O. F.; Li, Y.; Herbst, C.; Rupprecht, A. *J. Phys. Chem.* **1990**, *94*, 4655–4660.
(37) Tang, S. L.; McGhie, A. J.; Suna, A. *Phys. Rev. B* **1993**, *47*, 3850–3856.
(38) Yuan, J.; Shao, Z.; Gao, G. *Phys. Rev. Lett.* **1991**, *67*, 863–866.
(39) With the STM electronics available to us, $I-V$ curves can only be satisfactory performed on graphite. The relatively long periods for data adquisition as well as the application of positive and negative voltages during the ramp usually implies degradation of the membranes.

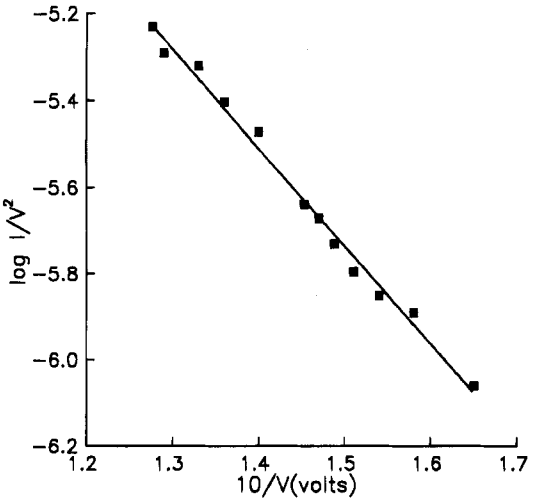

Figure 5. Typical logarithmic plot of I/V^2 versus $1/V$. The linear dependence is consistent with a field emission process described by the Fowler–Nordheim equation. The tip–substrate distance was defined by a bias voltage of −8 V and current of 0.34 pA.

The linear dependence of log I vs $1/V$ is characteristic of a field emission process described by the Fowler–Nordheim equation.[40]

$$I = AV^2 \exp\left(-6.85\phi^{3/2}\frac{S}{V}\right) \qquad (1)$$

where A is a factor that depends on the emitting area, V is the applied voltage, S is the tip–substrate distance, and ϕ is the emitter work function; distances are in nanometers and energies in electronvolts. Furthermore, I versus S measurements were also performed. From those curves, effective barrier heights of (3 ± 0.5 eV) were obtained. Those high values obtained in air also support a field emission process.[41]

The theory of Yuan, Shao, and Gao[38] proposes ions as the carriers for imaging biomolecules with STM. However, we are not aware of any ion-assisted conduction process that follows the Fowler–Nordheim dependence. Furthermore, we consider unlikely to have an experimental situation where the current has two components, ions and electrons and both of the same order of magnitude, one that applies when the tip is on the substrate (electrons) and the other on the membrane (ions). Besides, the existence of negative contrast and the observation of a reduction of the height measurement when several membranes piled on top of each other seem to be at variance with the theory presented in ref 38.

The model we propose attempts to explain the origin of the contrast and its dependence with tip–substrate separation (see Figure 6a). A realistic calculation of electron transport through the biomolecule has to include the complex structure of the proteins as well as their complicated energy surface for electron motion. This will require a computational power beyond our reach. However, we consider that insight about the dominant mechanism of contrast could be gained by using a simplified one-electron model for the electronic structure of proteins within the membrane.

The protein is replaced by an energy potential with an effective work function ϕ_m, a pseudoband of empty states above the fermi level of the substrate (ϕ_b), and a static

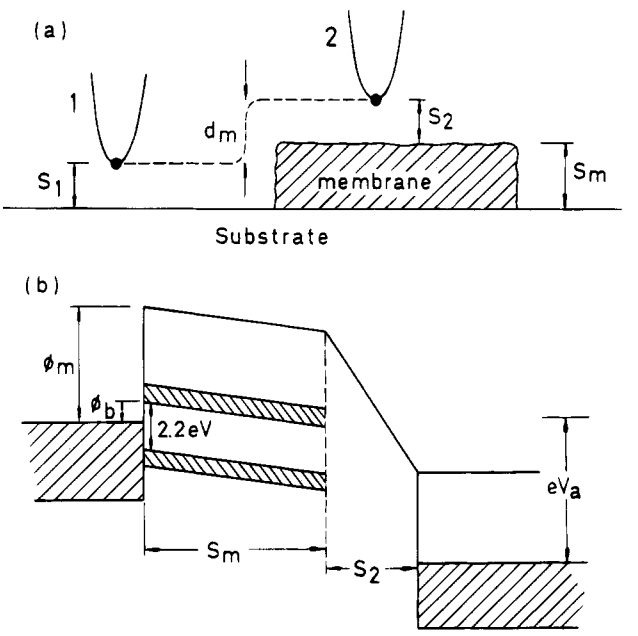

Figure 6. (a) Schematic representation of the experimental situation. The dashed line describes a hypothetical displacement of the tip for keeping the current constant when going from situation 1 (bare substrate) to situation 2 (over the membrane). (b) One-dimensional energy potential for the substrate–membrane–air gap–tip interface when there is an external voltage.

dielectric constant (K_m) (Figure 6b). The pseudoband of empty states is explained by the observation of a wide absorption band centered around 2.2 eV above the occupied molecular orbitals in the protein.[27] The effective barrier height could be related to the ionization potential of the protein. In the calculations we use $\phi_m = 7.5$ eV and $\phi_b = 0.5$ eV which corresponds to an ionization potential of 9.2 eV. The values of these parameters may affect the numerical results, but the behavior predicted by the model is not very sensitive to the values chosen.[42]

The contrast of the images is quantified by measuring the apparent height d_m of the membranes. This quantity can be calculated through

$$d_m = S_m + S_2 - S_1 \qquad (2)$$

S_m is the nominal thickness of the membrane as measured by other techniques (~5 nm). S_1 and S_2 are the tip–substrate and tip–membrane separations, respectively (Figure 6a). To calculate the dependence of the contrast with S_1, we impose that the current does not change when the tip moves from the substrate to the membrane (these experiments are performed in the constant current mode). We also assume that when the tip is over the membrane, the current is determined by the product of the transmission coefficients of the substrate–membrane and membrane–air interfaces. Each of these transmission coefficients is assumed to follow a Fowler–Nordheim-like law. Then, neglecting differences in the prefactors

$$\phi_s^{3/2}\frac{S_1}{V} = \phi_b^{3/2}\frac{S_m}{V_m} + (\phi_m - V_m)^{3/2}\frac{S_2}{V - V_m} \qquad (3)$$

where ϕ_s is the work function of the substrate.

Equation 3 assumes that electrons propagate as quasi-free particles or follow paths similar to those described in ref 35 in the pseudoband.

(40) Gomer, R. *Field emission and field ionization microscopy*; Harvard University Press: Cambridge, MA, 1961.
(41) Gómez-Herrero, J.; Gómez-Rodríguez, J. M.; García, R.; Baró, A. M. *J. Vac. Sci. Technol. A* **1990**, *8*, 445.
(42) Dielectric constants of proteins are not known with exactitude. Their estimated value is about 2–5. Here a value of 4 is taken.

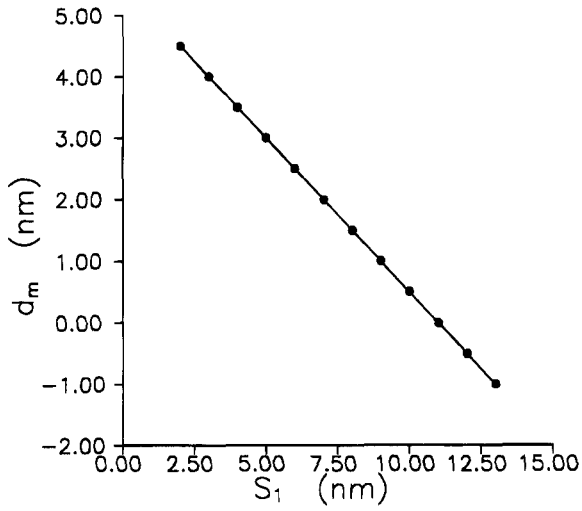

Figure 7. Apparent height versus tip–substrate separation. Positive values means the tip retracts when encountering the membrane. Negative values mean the tip moves toward the membrane. The calculation have been performed for $\phi_s = 5$ eV, $\phi_m = 7.5$ eV, V = −8 V, $K_m = 4$, and $S_m = 5$ nm.

The continuity conditions for the electrical field at the membrane surface imply

$$\frac{V_m}{S_m} = \frac{V}{K_m S_2 + S_m} \tag{4}$$

V_m and V_2 are the voltage drop in the membrane and in the air-gap region, respectively ($V = V_m + V_2$). A relationship between S_2 and S_1 can be derived by manipulating eqs 3 and 4. For $V_m < \phi_m$, the dependence of d_m with S_1 is expressed by

$$d_m = \left[\frac{3eV}{2K_m}\frac{\phi_m^{1/2}}{(\phi_m^{3/2} + \phi_b^{3/2})} + 1 - K_m\right]S_m - \left[\frac{\phi_s^{3/2}}{(\phi_m^{3/2} + K_m\phi_b^{3/2})} - 1\right]S_1 \tag{5}$$

From the calculations is obtained that the contrast is a property of the electrical field at the substrate–membrane interface (Figure 7). In particular the model reproduces the experimental data reported by Guckenberger et al.[22] and here that negative/positive contrast is a function of tip–substrate separation. This behavior has its origin in the competition between the position of the empty states, the thickness of the membrane, and its dielectric constant for controlling the emission. $\phi_b < \phi_s$ tends to decrease the barrier when the tip is over the membrane with respect to bare substrate. However, this effect may be compensated by $K_m > 1$, that decreases the voltage drop in the membrane, i.e., increases the barrier. What eventually tips the balance to positive or negative contrast is the electric field at the tip–membrane interface: higher fields, higher contrast.

This interpretation opens a new method for imaging insulating thin films and biomolecules at high resolution. The lateral resolution has two components (i) the geometry of the tip and (ii) the local variation of the effective barrier. This variation can be due to changes in chemical composition or to different packing of the molecules. The vertical resolution comes from the dependence of the electrical field with the tip–sample separation.[30]

Efforts for imaging at high-resolution organic molecules by field emission can be traced back to the work of Melmed and Muller.[43] Patterns of several different biomolecules were obtained by field emission microscopy (FEM).[40,43] However, the resulting image shapes were quite similar, i.e., independent of the morphology of the biomolecule, so the usefulness of field emission approaches for imaging biomolecules was questioned.[44]

Several factors could account for the difference between the present results and those reported by FEM. Here, electrons are emitted from relatively smooth electrodes. In FEM, electrons leave sharp tips of about radius of curvature 20 nm. The electrical fields, though in the same range, are different. We have used fields of about 1 V/nm while in FEM fields of 3 V/nm were used for imaging copper phthalocyanine. But, the main factor may be the difference in the operation of the STM and FEM.

V. Summary

In this paper we have characterized the dominant parameters for imaging uncoated purple membranes with the STM. These are the applied voltage, the current density, and the tip radius. We have imaged purple membrane patches with a vertical resolution of 0.7 nm and lateral of 15 nm. The membranes can be properly imaged for set currents below 2 pA and applied voltages above 5.5 V, negative polarities perferred. When both requirements are not met, to keep the current constant implies tip–membrane mechanical contact. This is often accompanied by disruption of the membrane and the removal of the proteins by the tip. This effect can be exploited to generate nanometer-scale manipulations of biological membranes.

To explain the observed contrast and its dependence with tip–substrate separation, a model based on field emission and on the existence of empty states in the proteins is elaborated. The experimental data and the calculations indicate a new physical mechanism for imaging at high resolution in a noncontact mode hydrated biomolecules and insulating thin films.

Acknowledgment. We thank P. Turina and G. Rayfield for the help in sample preparations and for valuable suggestions and R. Guckenberger, D. Dunlap, A. Gibson, and J. J. Sáenz for useful discussions and comments. R. G. has received financial support from the Ministerio de Educación y Ciencia (Spain) PB97-0016.

LA9406113

(43) Melmed, A. J.; Müller, E. W. *J. Chem. Phys.* **1958**, *29*, 1037–1041.

(44) Panitz, J. A.; Giaver, I. *Surf. Sci.* **1980**, *7*, 25–42.